environmental microbiology

Environmental Microbiology (2017) **19**(7), 2862–2872 doi:10.1111/1462-2920.13814

Type 4 pili are dispensable for biofilm development in the cyanobacterium *Synechococcus elongatus*

Elad Nagar,[1] Shaul Zilberman,[1] Eleonora Sendersky,[1] Ryan Simkovsky,[2] Eyal Shimoni,[3] Diana Gershtein,[4] Moshe Herzberg,[4] Susan S. Golden[2] and Rakefet Schwarz[1]*

[1]*The Mina and Everard Goodman Faculty of Life Sciences, Bar-Ilan University, Ramat-Gan, 5290002 Israel.*

[2]*Division of Biological Sciences, University of California, San Diego, La Jolla, CA 92093, USA.*

[3]*Weizmann Institute of Science, Electron Microscopy Unit, Rehovot, 7610001 Israel.*

[4]*The Department of Desalination & Water Treatment, Zuckerberg Institute for Water Research, Ben-Gurion University of the Negev, Sede Boqer Campus, Be'er Sheva 84990, Israel.*

Summary

The hair-like cell appendages denoted as type IV pili are crucial for biofilm formation in diverse eubacteria. The protein complex responsible for type IV pilus assembly is homologous with the type II protein secretion complex. In the cyanobacterium *Synechococcus elongatus* PCC 7942, the gene Synpcc7942_2071 encodes an ATPase homologue of type II/type IV systems. Here, we report that inactivation of Synpcc7942_2071 strongly affected the suite of proteins present in the extracellular milieu (exoproteome) and eliminated pili observable by electron microscopy. These results support a role for this gene product in protein secretion as well as in pili formation. As we previously reported, inactivation of Synpcc7942_2071 enables biofilm formation and suppresses the planktonic growth of *S. elongatus*. Thus, pili are dispensable for biofilm development in this cyanobacterium, in contrast to their biofilm-promoting function in type IV pili-producing heterotrophic bacteria. Nevertheless, pili removal is not required for biofilm formation as evident by a piliated mutant of *S. elongatus* that develops biofilms. We show that adhesion and timing of biofilm development differ between the piliated and non-piliated strains. The study demonstrates key differences in the process of biofilm formation between cyanobacteria and well-studied type IV pili-producing heterotrophic bacteria.

Received 21 February, 2017; revised 23 May, 2017; accepted 30 May, 2017. *For correspondence. E-mail Rakefet.Schwarz@biu.ac.il

Introduction

Pili, proteinaceous filaments that are found on the surface of bacterial cells, are involved in diverse functions, including competence for DNA uptake, motility and interaction with eukaryotic cell surfaces and subsequent pathogenesis (Giltner *et al.*, 2012; Hachani *et al.*, 2016). Numerous studies indicate that in heterotrophic bacteria that possess type IV pili (T4P), these structures promote biofilm formation (Mandlik *et al.*, 2008; Karatan and Watnick, 2009; Burrows, 2012; Chagnot *et al.*, 2013; Kostakioti *et al.*, 2013; Piepenbrink and Sundberg, 2016). For example, mutants of *Pseudomonas aeruginosa* PA14, which are impaired in biogenesis of T4P, support the involvement of these filaments in the formation of microcolonies, during the initial steps of a developing biofilm (O'Toole and Kolter, 1998). In addition, studies employing differentially fluorescently labeled wild type (WT) and T4P-mutant cells demonstrated that twitching motility, which is dependent on T4P, is essential for development of mushroom-like, mature multicellular biofilm structures (Klausen *et al.*, 2003; Barken *et al.*, 2008). T4P are also involved in *P. aeruginosa* migration, leading to the formation of a fibre-like polysaccharide matrix in biofilms (Wang *et al.*, 2013). Various *Escherichia coli* isolates employ cell appendages termed fimbriae for adhesion and biofilm formation; however, enteropathogenic *E. coli*, a type IV pilus-producing biotype, requires these pili for adherence to host cells and autoaggregation phenotypes (Bieber *et al.*, 1998). Additionally, type IV pili of the plant pathogens *Agrobacterium tumefaciens* and *Acidovorax avenae* subsp. citrulli are involved in adhesion to the host tissue and biofilm formation (Bahar *et al.*, 2009; Wang *et al.*, 2014).

Studies in cyanobacteria support a role for T4P in motility (e.g. phototaxis) and natural DNA competence (reviewed in Bhaya, 2004; Schuergers and Wilde, 2015). Components of the pilus and its assembly complex were identified in several species including *Synechocystis* sp.

PCC 6803 (Bhaya *et al*., 2000; Yoshihara *et al*., 2001) and *Nostoc punctiforme* (Duggan *et al*., 2007). Furthermore, the sigma factor SigF (Bhaya *et al*., 1999) and the RNA chaperone homolog Hfq (Schuergers *et al*., 2014) were shown to be involved in regulation of motility in *Synechocystis* PCC 6803. A modified type IV pilus-like system is involved in gliding motility of *N. punctiforme* (Khayatan *et al*., 2015).

Cyanobacteria are frequently found in biofilms, and often these communities impose a detrimental effect in various industrial applications, for example, by blocking flow through membranes used in desalination plants and by causing material decay of submersed objects (Baker and Dudley, 1998; Flemming, 2002). Phototrophic biofilms, however, may be useful in other processes (e.g., biofuel production, Gross *et al*., 2015; Heimann, 2016).

The molecular mechanisms that underlie cyanobacterial aggregation only recently attracted attention (Fisher *et al*., 2013; Jittawuttipoka *et al*., 2013; Schatz *et al*., 2013; Enomoto *et al*., 2014; Schwarzkopf *et al*., 2014; Enomoto *et al*., 2015; Oliveira *et al*., 2015a; Agostoni et al., 2016; Parnasa *et al*., 2016). We previously reported that the inactivation of Synpcc7942_2071 of the cyanobacterium *Synechococcus elongatus* PCC 7942 results in biofilm development in an otherwise planktonic strain (Schatz *et al*., 2013). The formation of a *bona fide* biofilm by the mutant strain indicates that a genetic program that underlies biofilm development exists in the laboratory strain and is constitutively inhibited.

The role of T4P in cyanobacterial biofilm development has not been investigated thus far. Here, we demonstrate that inactivation of the gene Synpcc7942_2071, which enables biofilm formation, strongly influenced the exo-proteome (proteins present in the extracellular milieu) and abrogated pili formation. Thus, in contrast to the biofilm-promoting role of pili in T4P-producing heterotrophic bacteria, these cellular appendages are dispensable for biofilm development in *S. elongatus*. In addition, we revealed that the inactivation of Synpcc7942_2479, which encodes a PilA-like protein, results in a piliated strain that forms biofilms under particular conditions.

Results and discussion

Inactivation of Synpcc7942_2071 affects the exo-proteome

The Synpcc7942_2071 gene encodes an ATPase homologue of type II secretion systems, denoted T2SE. Inactivation of this gene results in biofilm formation, in contrast to the WT strain of *S. elongatus*, which grows planktonically under standard laboratory conditions (Schatz *et al*., 2013). Analysis of extracellular proteins by gel electrophoresis followed by silver staining indicated that the Synpcc7942_2071 inactivated strain, T2SEΩ, has a dramatically reduced complement of extracellular proteins (Fig. 1A, also see Schatz *et al*., 2013), supporting a role for T2SE in protein secretion. To examine in greater detail the effect of inactivation of Synpcc7942_2071 on the exo-proteome, mass spectrometry analysis on conditioned media was employed. This analysis revealed proteins that are present at higher levels in extracellular fluids from WT as compared to T2SEΩ cultures, as well as those more prevalent in the mutant exo-proteome (Fig. 1B and Supporting Information).

Of the proteins more abundant in WT media, the largest change was observed for a protein of uncharacterized function encoded by Synpcc7942_0722, predicted by the Conserved Domain Database (CDD) to encode a RecT-like domain (Marchler-Bauer *et al*., 2015). A protein with a type IV N-terminus methylation site characteristic of pilin proteins (encoded by Synpcc7942_0048 and Synpcc7942_0049, hereafter Synpcc7942_0048/0049) was also highly enriched in the WT exo-proteome. Note that the sensitivity of silver staining of proteins separated by SDS-PAGE is inferior to MS analysis. For example, PilA was detected in conditioned medium from T2SEΩ by MS (Fig. 1B) but not by silver staining (Fig. 1A).

Clusters of Orthologous Groups (COGs) (Galperin *et al*., 2015) enrichment analysis demonstrated that the only enriched functional category in the exo-proteome of *S. elongatus* is that of unknown function, representing 55% of the proteins detected extracellularly compared to 43% of protein-encoding genes overall (p-value of 4.6×10^{-6}). Enrichment of functionally unknown proteins is a characteristic also noted for the exo-proteomes of *Anabaena* sp. PCC 7120 (Oliveira *et al*., 2015b) and *Synechocystis* sp. PCC 6803 (Oliveira *et al*., 2016). Other functional categories were not statistically significantly enriched (false discovery rate < 0.1) in the WT exo-proteome or the T2SEΩ exo-proteome compared to the total detected exo-proteome.

In contrast to the reduction in protein abundances observed by gel electrophoresis, some proteins were detected in significantly higher amounts in the exo-proteome of T2SEΩ as compared to WT (Fig. 1B and Supporting Information). Three of these proteins are unique to the exo-proteome of the mutant. The protein encoded by Synpcc7942_0122 is characterized by an EAL domain commonly associated with degradation of cyclic-di-GMP (c-di-GMP). The latter is a common second messenger that promotes biofilm development in heterotrophic bacteria (Kolter and Greenberg, 2006; Boyd and O'Toole, 2012; Povolotsky and Hengge, 2012; Sondermann *et al*., 2012; Romling *et al*., 2013), and recent studies support its involvement in cyanobacterial aggregation (Agostoni et al., 2016; Enomoto *et al*., 2015). It is possible that release of the protein encoded by Synpcc7942_0122 to the medium allows intracellular accumulation of c-di-GMP and, thus,

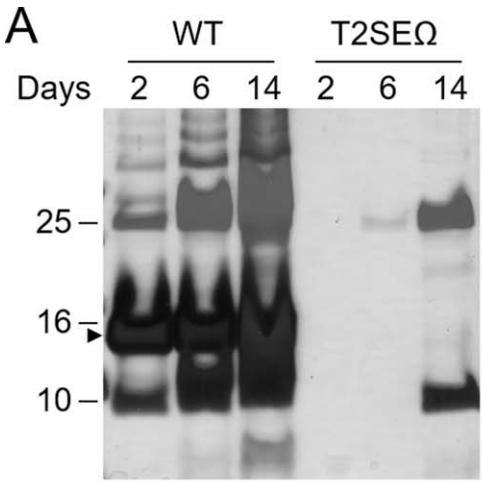

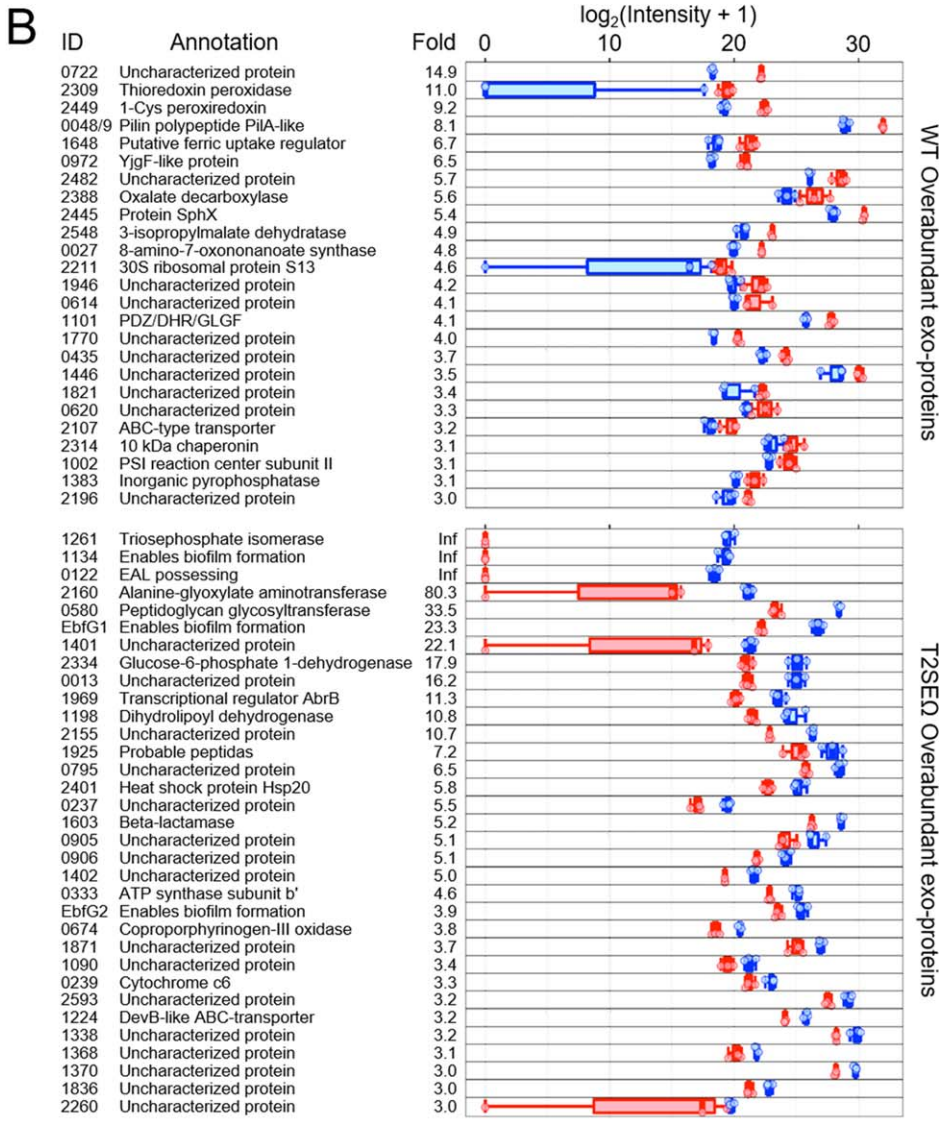

Fig. 1. Inactivation of Synpcc7942_2071 affects the exo-proteome.
A. Extracellular proteins from cultures of wild type (WT) and a mutant inactivated in Synpcc7942_2071 (T2SEΩ) at different stages of growth, analysed by gel electrophoresis followed by silver staining. Molecular weight markers are indicated in kDa on the left. Arrowhead indicates the ~ 15 kDa band in which the pilin protein, PilA, encoded by Synpcc7942_0048/0049 was detected (see the 'Experimental procedures' section for details). Each lane represents 3 ml of the original culture medium.
B. Analysis by MS of the entire exo-proteome of 2-day-old cultures indicated extracellular proteins more abundant in WT or in T2SEΩ (upper and lower panels, respectively). Shown are proteins with ratio of the levels between the strains $\geq$ 3.0 and *p*-value $\leq$ 0.05 as determined by Wilcox–Mann–Whitney tests. Numbers in the column 'Fold' indicate the fold change of the respective protein between WT versus mutant strain (upper panel) or mutant versus WT (lower panel). Numbers in the column 'ID' refer to specific four-number gene identities derived from Synpcc7942_xxxx gene designations. Intensity is proportional to the abundance of the peptide(s) detected. The intensity value of a peptide identified with multiple charge states is based on the highest signal amongst the charge states. Data are presented on a $\log_2$ scale. In particular cases, the amount of protein was below the detection limits of the instrument (intensity equals zero). To present all data on a log scale (including proteins for which intensity is zero), the value 1 was added to the intensity values (this addition is negligible relative to intensity levels of detected proteins, see Supplementary data for MS analysis). The genes Synpcc7942_0048 and Synpcc7942_0049 (indicated 0048/9) encode almost identical pilin proteins and were not distinguishable by the detected peptides. Inf (infinity) indicates that the protein was not detected in WT exo-proteome. *ebfG1* and *ebfG2* are previously un-annotated genes that enable biofilm formation and do not have a Synpcc number (see text, Parnasa *et al.*, 2016). Individual data points from three biological repeats are plotted as circles (WT = red, T2SEΩ = blue) overlaid on top of box plots, with the box representing the second and third quartiles, the bold line across the box indicating the median and the whisker bars representing the maximum and minimum values. [Color figure can be viewed at wileyonlinelibrary.com]

stimulation of biofilm formation by T2SEΩ. Three small proteins recently designated EbfG (enable biofilm formation with a GG secretion motif), previously shown to be important for biofilm development by T2SEΩ (Parnasa *et al.*, 2016), are enriched in the T2SEΩ exo-proteome: EbfG1 and EbfG2 are more abundant in T2SEΩ than in the WT, and EbfG4 (Synpcc7942_1134) was not detected in the WT exo-proteome at all (Fig. 1B). These data imply that enhanced secretion of a suite of proteins by the mutant is the consequence of T2SE impairment on cell function.

Triosephosphate isomerase (Synpcc7942_1261) is also found exclusively in the exo-proteome of the mutant. Interestingly, cell surface-associated triosephosphate isomerase is required for the adherence of *Staphylococcus aureus* to cells of the fungal pathogen, *Cryptococcus neoformans* (Ikeda *et al.*, 2007), and *Lactobacillus plantarum* to human Caco-2 colorectal cells (Ramiah *et al.*, 2008). Perhaps this enzyme is deposited to the outer surface of T2SEΩ where it mediates cell adhesion involved in biofilm development, although some of the molecules detach and are found in the extracellular fluids.

The exo-proteome potentially comprises secreted proteins as well as proteins released to the extracellular milieu by outer membrane vesicles or cell lysis. To assess the contribution of processes involving secretion across the cell membranes, the exo-proteome was analysed for the presence of signal peptides using several signal-prediction algorithms (see the 'Experimental procedures' section). These analyses indicate that the exo-proteome detected in this study is enriched three- to fivefold (depending on the particular algorithm used) over the predicted proteome for signal peptide-containing proteins (Table S1). However, the set of proteins more abundant either in WT or in T2SEΩ were not more enriched for signal peptide-possessing proteins than the total exo-proteome (Table S1). These data suggest that impairment of T2SE does not affect secretion machineries that rely on currently known or predictable signal peptides. Possibly, changes between the exo-proteome of WT and T2SEΩ result from activity of secretion processes that use non-traditional secretion signals or from other modes of protein release (e.g., lysis or outer membrane vesicles).

Inactivation of Synpcc7942_2071 abrogates pili formation

The Synpcc7942_2071 gene encodes T2SE, which is homologous to the PilB ATPase of pilus assembly complexes. Therefore, we examined whether inactivation of Synpcc7942_2071 affects cell piliation. Examination of negatively stained whole cells by transmission electron microscopy revealed WT cells with pili (Fig. 2A), whereas T2SEΩ lacks cell pili (Fig. 2C). In WT samples, bundles of pili detached from cells were also observed (Fig. 2B) in accordance with the presence of abundant pilin protein, PilA, in extracellular fluids from WT cultures [Fig. 1A (arrowhead) and B (WT:EΩ approximately eightfold)]. These pili bundles were not observed in T2SEΩ samples. Biofilm formation by the non-piliated T2SEΩ strain indicates that pili are not essential for this process in *S. elongatus*, in sharp contrast to their involvement in biofilm development in T4P-producing heterotrophic bacteria.

The higher abundance of some proteins in WT compared to T2SEΩ extracellular fluids suggests that inactivation of Synpcc7942_2071 impairs secretion processes while also abrogating pili formation. Thus, it is possible that the ATPase homologue encoded by Synpcc7942_2071 takes part in the following two different systems: a type II protein secretion complex and a T4P assembly apparatus. It is conceivable, however, that *S. elongatus* has a single machinery that carries out both functions, as has been demonstrated in other bacteria,

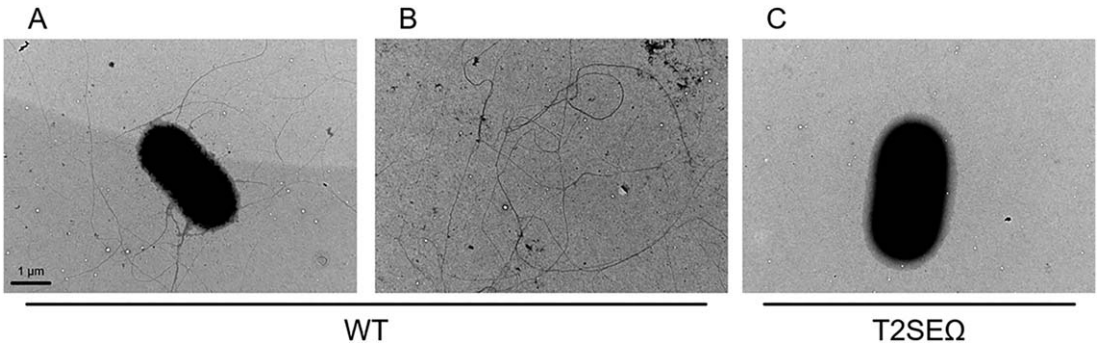

Fig. 2. Inactivation of Synpcc7942_2071 abrogates pili formation.
Transmission electron microscopy images following negative staining. Examination of wild type (WT) samples revealed cell pili (A), as well as bundles of pili detached from cells (B). The Synpcc7942_2071 inactivated strain, T2SEΩ, lacks pili (C). Bundles of pili were not observed in the case of T2SEΩ.

including *Vibrio cholera* (Kirn *et al*., 2003), *Dichelobacter nodosus* (Han *et al*., 2007), and *E. coli* (Sauvonnet *et al*., 2000).

Inactivation of Synpcc7942_2479 results in a piliated strain that forms biofilms under particular conditions

The structural protein comprising the cell pilus from many bacterial species, PilA, is produced as a pre-pilin precursor that undergoes maturation by removal of an N-terminal sequence in a process involving methylation (Wallden *et al*., 2010; Melville and Craig, 2013). Pilin proteins may not share overall high sequence identity, but the N-terminal sequence signature facilitates bioinformatics identification of PilA homologs. Using PilFind (Imam *et al*., 2011) for the prediction of T4P-like signal peptides and their pre-pilin peptidase methylation sites, we identified several *pilA* candidate genes: Synpcc7942_0048, Synpcc7942_0049, Synpcc7942_2479, Synpcc7942_2482, Synpcc7942_2484, Synpcc7942_2485, Synpcc7942_2590 and Synpcc7942_2591. These genes were previously reported by others as *pilA* candidates (Linhartova *et al*., 2014). We examined the effect of inactivation of the *pilA* candidate genes on biofilm development.

Synpcc7942_0048/0049 are adjacent genes (Fig. 3A) that encode PilA homologs with 98% amino acid identity. Deletion of both these genes simultaneously resulted in a non-piliated strain, PilA1 (Fig. 3B), that exhibited biofilm formation (Fig. 3C). However, biofilm development by this strain was not stable – biofilming was observed for several months, after which the strain grew planktonically. Therefore, the mutant was not further characterized.

Inactivation of Synpcc7942_2479 (Fig. 3A), encoding a pilin-like protein, yielded a piliated strain (Fig. 3B) dubbed PilA2. The PilA2 mutant exhibits delayed biofilm development compared to T2SEΩ (Fig. 3C). Assessment of the relative amount of chlorophyll in suspended cells as a measure of biofilm development indicated that T2SEΩ initiated biofilm formation (40% of the chlorophyll in suspended cells) by day 2 and formed a substantial biofilm by day 4 (only 10% of the chlorophyll in suspended cells). In contrast, PilA2 did not initiate biofilm formation until day 4 and required further time to develop a biofilm similar to T2SEΩ.

The biofilm assay described above (Fig. 3C) was performed in 50 ml cultures grown under continuous bubbling ('Experimental procedures' section). Apparently, biofilms of the PilA2 mutant formed under these conditions are similar to those exhibited by T2SEΩ (Fig. S1A). When grown under the same conditions but in 25 ml cultures, PilA2 grew planktonically whereas T2SEΩ formed robust biofilms. Likely, turbulent conditions in the 25 ml cultures prohibited biofilm development by the PilA2 strain, suggesting either less adhesive properties in the absence of this protein or buoyancy under these conditions due to the presence of pili.

Inactivation of additional *pilA* candidates (Synpcc7942_2482, Synpcc7942_2484, Synpcc7942_2485, Synpcc7942_2590 and Synpcc7942_2591) resulted in planktonically growing cells (Fig. S2).

In summary, deletion of Synpcc7942_0048/0049 (PilA1 strain) abrogated pili formation. This observation, together with the mass spectrometry data indicating abundance of the pilin protein encoded by Synpcc7942_0048/0049 in WT compared to the non-piliated mutant, T2SEΩ, support the suggestion that Synpcc7942_0048/0049 encode the major pilus subunit of *S. elongatus*. Inactivation of Synpcc7942_2479 (PilA2 strain) resulted in a piliated strain that is capable of forming biofilms; however, biofilm formation occurs only under particular growth conditions and is delayed compared to T2SEΩ. Although biofilm development differs between the piliated mutant (PilA2) and the strain that lacks pili (T2SEΩ), the observation that a piliated strain does form biofilms indicates that elimination of pili is not compulsory for biofilm development.

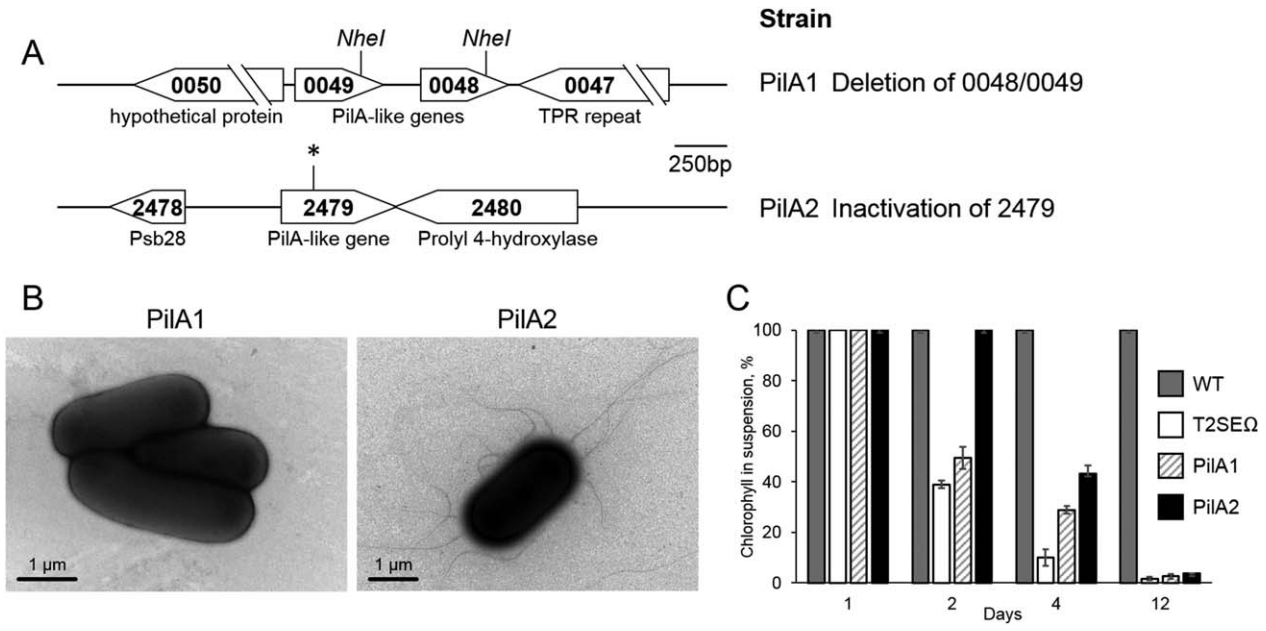

Fig. 3. (A) Maps of the genomic regions of *pilA*-candidate genes, the inactivation of which resulted in biofilm formation. The strain PilA1 was obtained by deletion of the fragment between the *NheI* sites. PilA2 was constructed by inactivation of Synpcc7942_2479 (asterisk denotes the transposon insertion site). (B) Transmission electron microscopy images following negative staining of PilA1 and PilA2. PilA1 lacks cell pili, in contrast to the pileated PilA2 strain. Cell clustering of the PilA1 strain likely represents an artefact of the preparation, since examination of cultures of this strain by fluorescence microscopy revealed individual cells. (C) Biofilm development in T2SEΩ PilA1 and PilA2 mutants. Chlorophyll in suspended cells as a function of growth time in cultures of wild type (WT), T2SEΩ, PilA1 and the PilA2 mutants. Graph shows averages and standard deviations of three technical repeats. Late onset of biofilm development in PilA2 compared to T2SEΩ was reproducibly observed in independent experiments, however, in different experiments T2SEΩ started biofilm development either on day 2 or day 3. For an as yet unknown reason, the biofilming phenotype of PilA1 was not stable, and after several months, the mutant grew planktonically.

Absence of pili correlates with fast cell sedimentation

Pili are known to be involved in cell movement. We therefore tested whether impairment of T2SE, which eliminates piliation (Fig. 2C), affects the ability of the cells to remain suspended. In contrast to marine cyanobacterial strains that exhibit swimming motility (Waterbury *et al.*, 1985; Pitta and Berg, 1995; McCarren and Brahamsha, 2009), *S. elongatus* was not reported to swim in liquid or to exhibit motility on soft agar. However, WT cells remain largely suspended in liquid by an unknown mechanism. To compare the ability of WT and mutant cells to stay buoyant, we used fluorescence microscopy to follow the number of cells accumulating at the bottom of a petri-dish over a time course. This analysis indicated enhanced sedimentation of T2SEΩ cells compared to the WT (Fig. 4). The faster sedimentation of T2SEΩ may result from changes in friction coefficient due to the absence of pili. It is also possible that the pili form a physical network that assists WT cells to remain buoyant.

The correlation between fast cell sedimentation and biofilm development in T2SEΩ encouraged us to test additional rapidly sedimenting mutants for biofilm development. We examined 68 transposon insertion mutants, which in the course of a high throughput screen of a genomic inactivation library of *S. elongatus* (Holtman *et al.*, 2005; Chen *et al.*, 2012) were identified as having non-suspended phenotypes. Biofilm development was observed by only four of these 68 mutants (Table S2).

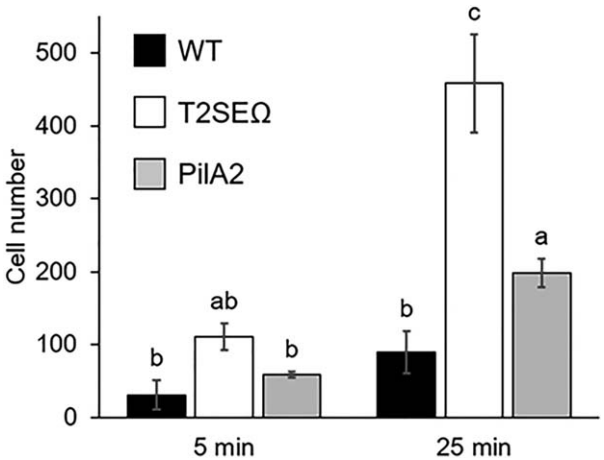

Fig. 4. Cell sedimentation in wild type (WT), T2SEΩ and PilA2 cultures. Accumulation of cells at the bottom of a petri-dish as revealed by fluorescence microscopy. Graph shows averages and standard deviations of at least three independent biological repetitions. Different letters assign statistical significance (p-value < 0.05).

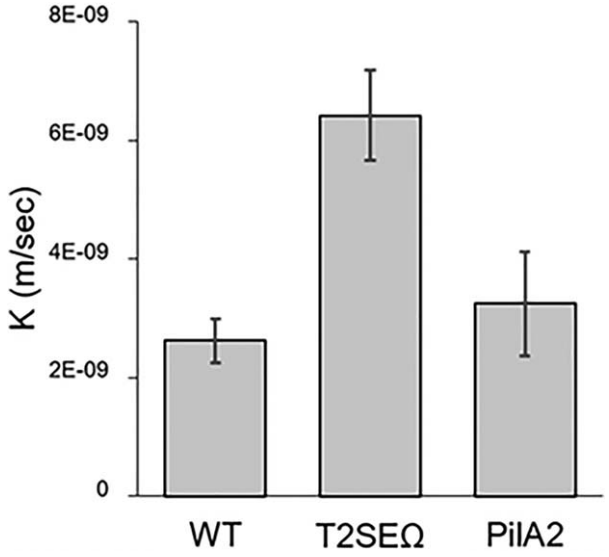

Fig. 5. Deposition rate onto a glass slide of wild type (WT), T2SEΩ and PilA2 cells.
Cell attachment was examined in a flow cell. K_0 is the transfer rate coefficient (see the 'Experimental procedures' section). Graph shows averages and standard deviations of three independent biological repetitions. Two-way analysis of variance indicated significant differences between T2SEΩ and WT or PilA2 (p-value < 0.05).

These strains were inactivated in the following genes: (i) Synpcc7942_2069 encoding a PilC homolog. We previously reported that inactivation of this gene leads to biofilm development (Schatz *et al.*, 2013). (ii) Synpcc7942_2479 encoding a pilin protein homolog (the mutant is denoted here as PilA2). (iii) Synpcc7942_2452 encoding a PilN homolog. (iv) Synpcc7942_0862 encoding a protein of unknown function. The observation that very few of the sedimenting mutants form biofilms indicates that increased sedimentation, by itself, is not sufficient for biofilm formation. Likely, biofilms develop only when the strain is capable of strong adhesion to the substratum or able to activate a biofilm formation program involving the secretion of the EbfG genes (Parnasa *et al.*, 2016).

We specifically examined cell sedimentation in the PilA2 strain. This strain sediments much slower than T2SEΩ but exhibits enhanced sedimentation compared to WT cells (Fig 4). It is possible that a change in pilus composition altered its function in the PilA2 strain, thus affecting sedimentation.

Absence of pili correlates with strong cell adhesion

To further characterize the process of biofilm development in the piliated (PilA2) and non-piliated (T2SEΩ) strains, we compared adhesion to the substratum, a crucial step of biofilm development. Deposition of cells onto a glass slide, which was examined in a flow cell ('Experimental procedures' section) revealed higher deposition rate for T2SEΩ compared to WT (Fig. 5). The PilA2 mutant, however, did not exhibit significantly different deposition than WT cells. Conceivably, removal of the pili exposes an adhesion molecule or surface, thereby allowing strong attachment to the substratum and promoting biofilm formation. It is also possible that the pili confer cell motility resulting in detachment of loosely associated cells. As noted above, the PilA2 strain formed biofilms under continuous bubbling in 50 ml but not in 25 ml cultures. These observations together with the differences in deposition rate suggest that only particular conditions support sufficiently strong attachment of PilA2 cells to allow biofilm development.

In conclusion, this study demonstrates that abrogation of pili formation promotes biofilm development in *S. elongatus* PCC 7942. This is in stark contrast to T4P-producing heterotrophic bacteria, where pili promote biofilm formation. Removal of pili, however, is not essential for biofilm development, although our data suggest that the presence of pili reduces sedimentation, interferes with adhesion, and consequently slows down the kinetics of biofilm formation. Additionally, inactivation of Synpcc7942_2071 affects the exo-proteome and eliminates cell pili, suggesting that the ATPase homologue encoded by this gene takes part in both protein secretion as well as pilus formation.

Experimental procedures

Strains, culture conditions, biofilm quantification and electron microscopy

Growth of *S. elongatus* PCC 7942 and all derived strains, as well as quantification of biofilms, were described previously (Parnasa *et al.*, 2016). Routinely, cells were grown in 25 ml cultures; however, because the PilA2 mutant did not form biofilms under these conditions, all strains were grown in 50 ml cultures for experiments involving this mutant. Molecular manipulations are summarized in Table S3. Where indicated, cloning was done by seamless assembly (Taton *et al.*, 2014). To observe pili by transmission electron microscopy, three day old cultures that had not yet initiated biofilm formation were diluted to an OD_{750} of 0.5. Samples (4 μl) were negatively stained with 1% uranyl acetate. Images were acquired in a Tecnai T12 or Tecnai Spirit transmission electron microscope (FEI, Holland, Netherlands) operating at 120 kV, using either a 2k × 2k F224HD CCD camera (TVIPS GmbH, Gauting, Germany) or a 2k × 2k Eagle CCD camera (FEI).

Analysis of extracellular fluids

Analysis of extracellular fluids by SDS-PAGE and silver staining was described previously (Schatz *et al.*, 2013). To analyse the ~15 kDa band (e.g., Fig. 1A, WT), this region was excised from the silver-stained gel and examined by mass spectrometry at The Smoler Protein Research Center, Technion, Israel Institute of Technology. The proteins in the gel were reduced with 3 mM dithiothreitol (60°C for 30 min), modified with

10 mM iodoacetamide in 100 mM ammonium bicarbonate (in the dark, room temperature for 30 min), and digested in 10% acetonitrile and 10 mM ammonium bicarbonate with modified trypsin (Promega, Madison, WI, USA) overnight at 37°C. The resulting tryptic peptides were resolved by reverse-phase chromatography on 0.075 mm × 200 mm fused silica capillaries (J&W Agilent, Santa Clara, CA, USA) packed with Reprosil reversed phase material (Dr Maisch GmbH, Ammerbuch-Entringen, Germany). The peptides were eluted with linear gradients of 5–45% (65 min) and 95% (15 min) acetonitrile with 0.1% formic acid in water at flow rates of 0.25 μl min^{-1}. Mass spectrometry was performed by an ion-trap mass spectrometer (OrbitrapXL; ThermoFisher, Waltham, MA, USA) in positive, repetitive full scan mode followed by collision induced dissociation (CID) of the five most dominant ions selected from the first MS scan. The mass spectrometry data were analysed using Protein Discoverer 1.3 (ThermoFisher) using the SEQUEST search engine searching against the *S. elongatus* protein database. Peptide- and protein-level false discovery rates (FDRs) were filtered to 1% using the target-decoy strategy.

In addition, examination of the entire exo-proteome of 2-day-old cultures by mass spectrometry was done at the de Botton Institute for Protein Profiling at The Nancy and Stephen Grand Israel National Center for Personalized Medicine (Weizmann Institute of Science). This analysis was performed as previously described (Parnasa *et al*., 2016), with the exception that trypsin digestion was not followed by a chymotrypsin digest and 'Discovery mode' was used rather than 'Targeted analysis'. Statistical analysis on protein intensities in WT versus T2SEΩ proteomes used the Mann–Whitney *U* test, a non-parametric test, based on the expectation that the data is not normally distributed, as performed previously (Parnasa *et al*., 2016). For enrichment analysis, COGs, functional categories and signal peptide predictions, data were amassed from appropriate sources (Dilks *et al*., 2003; Bendtsen *et al*., 2005; Kall *et al*., 2007; Imam *et al*., 2011; Petersen *et al*., 2011; Pundhir and Kumar, 2011; Chen *et al*., 2017; Fujisawa *et al*., 2017) (see Supporting Information). Significant enrichment was determined using the one-sided Fisher's exact test, with a false discovery rate calculated from *p*-values of < 0.1 as the threshold for significance.

Assessment of cell sedimentation and cell adherence

Cell sedimentation. Two day old cultures that had not yet initiated biofilm formation were diluted to an OD_{750} of 1.0. A glass bottom 6-well plate (MatTak, 0.13 mm untreated borosilicate glass) was placed on the stage of an Axio Observer Z1 (Zeiss, Oberkochen, Germany) microscope and 6 ml of culture was transferred into a particular well to follow cell sedimentation. Images were recorded following 5 and 25 min (Objective – plan; apochromat 100x; reflector – 45 texas red. Exposure time – 200 ms, image size – 86.69 μm × 66.05 μm, camera – Hdcam). Images were analysed with ImageJ using the 'Analyze Particles\ function with manual corrections.

Cell adherence. Initial experiments indicated no differences between 2-day-old cultures of WT, T2SEΩ and PilA2. Therefore, 4-day-old planktonic cells were used for the analysis. Cultures were centrifuged (3500 × *g*, 15 min), washed twice with growth medium lacking the ferric ammonium citrate and citric acid components (hereafter, background solution), and re-suspended in this solution to an OD_{750} of 0.1. Deposition was assessed using a rectangular flow cell system (cat# 31–010; Glycotech, Gaithersburg, MD), placed on the stage of an upright fluorescence microscope (Nikon Eclipse LV100) equipped with 20X/0.45 WD 8.2–6.9 objective. The flow cell was assembled by attaching the deck together with a rubber gasket and a glass slide (Fig. S3), sealing it with a thin layer of vacuum grease. This construct formed an inner chamber 6 cm × 1 cm × 0.0762 cm in size. The inlet of the flow cell was attached to a 60 ml syringe pump keeping a flow rate of bacterial suspension of 0.2 ml min^{-1}. At least five images at each time point in different places of the glass slide were acquired with a Nikon Digital Sight (DS-2MBW) camera after 5, 15 and 30 min of bacterial injection. The number of cells attached to the surface was counted and the bacterial transfer rate coefficients (k) in m s^{-1} were determined as:

$$k = \frac{J}{C_0}$$

where J is the bacterial deposition flux (cells s^{-1} m^{-2}), and C_0 is the initial bacterial bulk concentration (cells m^{-3}). J was determined from the linear slope of the number of deposited cells versus time (normalized by the microscope viewing area, 320 μm × 120 μm).

Prior to deposition experiments, the glass slides were cleaned in a two-step process with 4 M hydrochloric acid and 1 M sodium hydroxide. Slides were thoroughly rinsed with deionized water after each step. The deposition experiments were carried out in the following series of injection stages: (i) deionized water for 15 min; (ii) background solution for 15 min; (iii) cyanobacterial culture (adjusted to an OD_{750} of 0.1) for 5 min; (iv) background solution for 3 min (removal of loosely attached cells); and (v) cell staining by addition of 2 ml of 0.04 mM propodium iodide. After 10 min, images of deposited cells were acquired while injecting background solution into the flow cell. Stages (iv) and (v) as well as image acquiring were repeated after further injection of a cyanobacterial culture for 10 and 15 min. Statistical analysis was done using two-way analysis of variance.

Acknowledgements

Studies in the laboratories of Rakefet Schwarz and Susan Golden were supported by the program of the National Science Foundation and the US-Israel Binational Science Foundation (NSF-BSF 2012823). This study was also supported by a grant from the Israel Science Foundation (ISF 1406/14) to Rakefet Schwarz. We thank Yishai Levin and Alon Savidor at the de Botton Institute for Protein Profiling, The Nancy and Stephen Grand Israel National Center for Personalised Medicine (Weizmann Institute of Science) and Tamar Ziv at The Smoler Protein Research Center (Technion, Israel Institute of Technology) for mass spectrometry analyses.

References

Agostoni, M., Waters, C.M., and Montgomery, B.L. (2016) Regulation of biofilm formation and cellular buoyancy

through modulating intracellular cyclic di-GMP levels in engineered cyanobacteria. *Biotechnol Bioeng* **113:** 311–319.

Bahar, O., Goffer, T., and Burdman, S. (2009) Type IV Pili are required for virulence, twitching motility, and biofilm formation of *Acidovorax avenae* subsp. citrulli. *Mol Plant Microb Interact* **22:** 909–920.

Baker, J.S., and Dudley, L.Y. (1998) Biofouling in membrane systems – a review. *Desalination* **118:** 81–89.

Barken, K.B., Pamp, S.J., Yang, L., Gjermansen, M., Bertrand, J.J., Klausen, M., *et al*. (2008) Roles of type IV pili, flagellum-mediated motility and extracellular DNA in the formation of mature multicellular structures in *Pseudomonas aeruginosa* biofilms. *Environ Microbiol* **10:** 2331–2343.

Bendtsen, J.D., Kiemer, L., Fausboll, A., and Brunak, S. (2005) Non-classical protein secretion in bacteria. *BMC Microbiol* **5:** 58.

Bhaya, D. (2004) Light matters: phototaxis and signal transduction in unicellular cyanobacteria. *Mol Microbiol* **53:** 745–754.

Bhaya, D., Watanabe, N., Ogawa, T., and Grossman, A.R. (1999) The role of an alternative sigma factor in motility and pilus formation in the cyanobacterium *Synechocystis* sp. strain PCC6803. *Proc Natl Acad Sci USA* **96:** 3188–3193.

Bhaya, D., Bianco, N.R., Bryant, D., and Grossman, A. (2000) Type IV pilus biogenesis and motility in the cyanobacterium *Synechocystis* sp. PCC6803. *Mol Microbiol* **37:** 941–951.

Bieber, D., Ramer, S.W., Wu, C.Y., Murray, W.J., Tobe, T., Fernandez, R., and Schoolnik, G.K. (1998) Type IV pili, transient bacterial aggregates, and virulence of enteropathogenic *Escherichia coli*. *Science* **280:** 2114–2118.

Boyd, C.D., and O'Toole, G.A. (2012) Second messenger regulation of biofilm formation: breakthroughs in understanding c-di-GMP effector systems. *Annu Rev Cell Dev Biol* **28:** 439–462.

Burrows, L.L. (2012) *Pseudomonas aeruginosa* twitching motility: type IV pili in action. *Annu Rev Microbiol* **66:** 493–520.

Chagnot, C., Zorgani, M.A., Astruc, T., and Desvaux, M. (2013) Proteinaceous determinants of surface colonization in bacteria: bacterial adhesion and biofilm formation from a protein secretion perspective. *Front Microbiol* **4:** 303.

Chen, I.A., Markowitz, V.M., Chu, K., Palaniappan, K., Szeto, E., Pillay, M., *et al*. (2017) IMG/M: integrated genome and metagenome comparative data analysis system. *Nucl Acids Res* **45:** D507–D516.

Chen, Y. H.C., Taton, A., and Golden, S.S. (2012) Functional analysis of the *Synechococcus elongatus* PCC 7942 genome – functional genomics and evolution of photosynthetic systems. *In Advances in Photosynthesis and Respiration*. Vol. 33. Burnap, R., and Vermaas, W. (eds). Netherlands: Springer, pp. 119–137.

Dilks, K., Rose, R.W., Hartmann, E., and Pohlschroder, M. (2003) Prokaryotic utilization of the twin-arginine translocation pathway: a genomic survey. *J Bacteriol* **185:** 1478–1483.

Duggan, P.S., Gottardello, P., and Adams, D.G. (2007) Molecular analysis of genes in *Nostoc punctiforme* involved in pilus biogenesis and plant infection. *J Bacteriol* **189:** 4547–4551.

Enomoto, G., Ni-Ni-Win, Narikawa, R., and Ikeuchi, M. (2015) Three cyanobacteriochromes work together to form a light color-sensitive input system for c-di-GMP signaling of cell aggregation. *Proc Natl Acad Sci USA* **112:** 8082–8087.

Enomoto, G., Nomura, R., Shimada, T., Ni-Ni-Win, Narikawa, R., and Ikeuchi, M. (2014) Cyanobacteriochrome SesA is a diguanylate cyclase that induces cell aggregation in *Thermosynechococcus*. *J Biol Chem* **289:** 24801–24809.

Fisher, M.L., Allen, R., Luo, Y., and Curtiss, R. 3rd (2013) Export of extracellular polysaccharides modulates adherence of the cyanobacterium *Synechocystis*. *PLoS One* **8:** e74514.

Flemming, H.C. (2002) Biofouling in water systems – cases, causes and countermeasures. *Appl Microbiol Biotechnol* **59:** 629–640.

Fujisawa, T., Narikawa, R., Maeda, S.I., Watanabe, S., Kanesaki, Y., Kobayashi, K., *et al*. (2017) CyanoBase: a large-scale update on its 20th anniversary. *Nucl Acids Res* **45:** D551–D554.

Galperin, M.Y., Makarova, K.S., Wolf, Y.I., and Koonin, E.V. (2015) Expanded microbial genome coverage and improved protein family annotation in the COG database. *Nucl Acids Res* **43:** D261–D269.

Giltner, C.L., Nguyen, Y., and Burrows, L.L. (2012) Type IV pilin proteins: versatile molecular modules. *Microbiol Mol Biol Rev* **76:** 740–772.

Gross, M., Jarboe, D., and Wen, Z. (2015) Biofilm-based algal cultivation systems. *Appl Microbiol Biotechnol* **99:** 5781–5789.

Hachani, A., Wood, T.E., and Filloux, A. (2016) Type VI secretion and anti-host effectors. *Curr Opin Microbiol* **29:** 81–93.

Han, X., Kennan, R.M., Parker, D., Davies, J.K., and Rood, J.I. (2007) Type IV fimbrial biogenesis is required for protease secretion and natural transformation in *Dichelobacter nodosus*. *J Bacteriol* **189:** 5022–5033.

Heimann, K. (2016) Novel approaches to microalgal and cyanobacterial cultivation for bioenergy and biofuel production. *Curr Opin Biotechnol* **38:** 183–189.

Holtman, C.K., Chen, Y., Sandoval, P., Gonzales, A., Nalty, M.S., Thomas, T.L., *et al*. (2005) High-throughput functional analysis of the *Synechococcus elongatus* PCC 7942 genome. *DNA Res* **12:** 103–115.

Ikeda, R., Saito, F., Matsuo, M., Kurokawa, K., Sekimizu, K., Yamaguchi, M., and Kawamoto, S. (2007) Contribution of the mannan backbone of cryptococcal glucuronoxylomannan and a glycolytic enzyme of *Staphylococcus aureus* to contact-mediated killing of *Cryptococcus neoformans*. *J Bacteriol* **189:** 4815–4826.

Imam, S., Chen, Z., Roos, D.S., and Pohlschroder, M. (2011) Identification of surprisingly diverse type IV pili, across a broad range of gram-positive bacteria. *PLoS One* **6:** e28919.

Jittawuttipoka, T., Planchon, M., Spalla, O., Benzerara, K., Guyot, F., Cassier-Chauvat, C., and Chauvat, F. (2013) Multidisciplinary evidences that *Synechocystis* PCC6803 exopolysaccharides operate in cell sedimentation and protection against salt and metal stresses. *PLoS ONE* **8:** e55564.

Kall, L., Krogh, A., and Sonnhammer, E.L. (2007) Advantages of combined transmembrane topology and signal peptide prediction – the Phobius web server. *Nucl Acids Res* **35:** W429–W432.

Karatan, E., and Watnick, P. (2009) Signals, regulatory networks, and materials that build and break bacterial biofilms. *Microbiol Mol Biol Rev* **73:** 310–347.

Khayatan, B., Meeks, J.C., and Risser, D.D. (2015) Evidence that a modified type IV pilus-like system powers gliding motility and polysaccharide secretion in filamentous cyanobacteria. *Mol Microbiol* **98:** 1021–1036.

Kirn, T.J., Bose, N., and Taylor, R.K. (2003) Secretion of a soluble colonization factor by the TCP type 4 pilus biogenesis pathway in *Vibrio cholerae*. *Mol Microbiol* **49:** 81–92.

Klausen, M., Heydorn, A., Ragas, P., Lambertsen, L., Aaes-Jorgensen, A., Molin, S., and Tolker-Nielsen, T. (2003) Biofilm formation by *Pseudomonas aeruginosa* wild type, flagella and type IV pili mutants. *Mol Microbiol* **48:** 1511–1524.

Kolter, R., and Greenberg, E.P. (2006) Microbial sciences – the superficial life of microbes. *Nature* **441:** 300–302.

Kostakioti, M., Hadjifrangiskou, M., and Hultgren, S.J. (2013) Bacterial biofilms: development, dispersal, and therapeutic strategies in the dawn of the postantibiotic era. *Cold Spring Harb Perspect Med* **3:** a010306.

Linhartova, M., Bucinska, L., Halada, P., Jecmen, T., Setlik, J., Komenda, J., and Sobotka, R. (2014) Accumulation of the type IV prepilin triggers degradation of SecY and YidC and inhibits synthesis of Photosystem II proteins in the cyanobacterium *Synechocystis* PCC 6803. *Mol Microbiol* **93:** 1207–1223.

Mandlik, A., Swierczynski, A., Das, A., and Ton-That, H. (2008) Pili in Gram-positive bacteria: assembly, involvement in colonization and biofilm development. *Trends Microbiol* **16:** 33–40.

Marchler-Bauer, A., Derbyshire, M.K., Gonzales, N.R., Lu, S., Chitsaz, F., Geer, L.Y., *et al*. (2015) CDD: NCBI's conserved domain database. *Nucl Acids Res* **43:** D222–22D226.

McCarren, J., and Brahamsha, B. (2009) Swimming motility mutants of marine *Synechococcus* affected in production and localization of the S-layer protein SwmA. *J Bacteriol* **191:** 1111–1114.

Melville, S., and Craig, L. (2013) Type IV pili in Gram-positive bacteria. *Microbiol Mol Biol Rev* **77:** 323–341.

O'Toole, G.A., and Kolter, R. (1998) Flagellar and twitching motility are necessary for *Pseudomonas aeruginosa* biofilm development. *Mol Microbiol* **30:** 295–304.

Oliveira, P., Pinto, F., Pacheco, C.C., Mota, R., and Tamagnini, P. (2015a) HesF, an exoprotein required for filament adhesion and aggregation in *Anabaena* sp PCC 7120. *Environ Microbiol* **17:** 1631–1648.

Oliveira, P., Martins, N.M., Santos, M., Couto, N.A., Wright, P.C., and Tamagnini, P. (2015b) The *Anabaena* sp. PCC 7120 exoproteome: taking a peek outside the box. *Life (Basel)* **5:** 130–163.

Oliveira, P., Martins, N.M., Santos, M., Pinto, F., Buttel, Z., Couto, N.A., *et al*. (2016) The versatile TolC-like Slr1270 in the cyanobacterium *Synechocystis* sp. PCC 6803. *Environ Microbiol* **18:** 486–502.

Parnasa, R., Nagar, E., Sendersky, E., Reich, Z., Simkovsky, R., Golden, S., and Schwarz, R. (2016) Small secreted proteins enable biofilm development in the cyanobacterium *Synechococcus elongatus*. *Sci Rep* **6:** 32209.

Petersen, T.N., Brunak, S., von Heijne, G., and Nielsen, H. (2011) SignalP 4.0: discriminating signal peptides from transmembrane regions. *Nat Methods* **8:** 785–786.

Piepenbrink, K.H., and Sundberg, E.J. (2016) Motility and adhesion through type IV pili in Gram-positive bacteria. *Biochem Soc Trans* **44:** 1659–1666.

Pitta, T.P., and Berg, H.C. (1995) Self-electrophoresis is not the mechanism for motility in swimming cyanobacteria. *J Bacteriol* **177:** 5701–5703.

Povolotsky, T.L., and Hengge, R. (2012) 'Life-style' control networks in *Escherichia coli*: signaling by the second messenger c-di-GMP. *J Biotechnol* **160:** 10–16.

Pundhir, S., and Kumar, A. (2011) SSPred: a prediction server based on SVM for the identification and classification of proteins involved in bacterial secretion systems. *Bioinformation* **6:** 380–382.

Ramiah, K., van Reenen, C.A., and Dicks, L.M. (2008) Surface-bound proteins of *Lactobacillus plantarum* 423 that contribute to adhesion of Caco-2 cells and their role in competitive exclusion and displacement of *Clostridium sporogenes* and *Enterococcus faecalis*. *Res Microbiol* **159:** 470–475.

Romling, U., Galperin, M.Y., and Gomelsky, M. (2013) Cyclic di-GMP: the first 25 years of a universal bacterial second messenger. *Microbiol Mol Biol Rev* **77:** 1–52.

Sauvonnet, N., Vignon, G., Pugsley, A.P., and Gounon, P. (2000) Pilus formation and protein secretion by the same machinery in *Escherichia coli*. *EMBO J* **19:** 2221–2228.

Schatz, D., Nagar, E., Sendersky, E., Parnasa, R., Zilberman, S., Carmeli, S., *et al*. (2013) Self-suppression of biofilm formation in the cyanobacterium *Synechococcus elongatus*. *Environ Microbiol* **15:** 1786–1794.

Schuergers, N., and Wilde, A. (2015) Appendages of the cyanobacterial cell. *Life (Basel)* **5:** 700–715.

Schuergers, N., Ruppert, U., Watanabe, S., Nurnberg, D.J., Lochnit, G., Dienst, D., *et al*. (2014) Binding of the RNA chaperone Hfq to the type IV pilus base is crucial for its function in *Synechocystis* sp. PCC 6803. *Mol Microbiol* **92:** 840–852.

Schwarzkopf, M., Yoo, Y.C., Hueckelhoven, R., Park, Y.M., and Proels, R.K. (2014) Cyanobacterial Phytochrome2 regulates the heterotrophic metabolism and has a function in the heat and high-light stress response. *Plant Physiol* **164:** 2157–2166.

Sondermann, H., Shikuma, N.J., and Yildiz, F.H. (2012) You've come a long way: c-di-GMP signaling. *Curr Opin Microbiol* **15:** 140–146.

Taton, A., Unglaub, F., Wright, N.E., Zeng, W.Y., Paz-Yepes, J., Brahamsha, B., *et al*. (2014) Broad-host-range vector system for synthetic biology and biotechnology in cyanobacteria. *Nucl Acids Res* **42:** e136.

Wallden, K., Rivera-Calzada, A., and Waksman, G. (2010) Type IV secretion systems: versatility and diversity in function. *Cell Microbiol* **12:** 1203–1212.

Wang, S., Parsek, M.R., Wozniak, D.J., and Ma, L.Z. (2013) A spider web strategy of type IV pili-mediated migration to build a fibre-like Psl polysaccharide matrix in *Pseudomonas aeruginosa* biofilms. *Environ Microbiol* **15:** 2238–2253.

Wang, Y., Haitjema, C.H., and Fuqua, C. (2014) The Ctp type IVb pilus locus of *Agrobacterium tumefaciens* directs formation of the common pili and contributes to reversible surface attachment. *J Bacteriol* **196:** 2979–2988.

Waterbury, J.B., Willey, J.M., Franks, D.G., Valois, F.W., and Watson, S.W. (1985) A cyanobacterium capable of swimming motility. *Science* **230:** 74–76.

Yoshihara, S., Geng, X., Okamoto, S., Yura, K., Murata, T., Go, M., *et al.* (2001) Mutational analysis of genes involved in pilus structure, motility and transformation competency in the unicellular motile cyanobacterium *Synechocystis* sp. PCC 6803. *Plant Cell Physiol* **42:** 63–73.

Supporting information

Additional Supporting Information may be found in the online version of this article at the publisher's web-site.

Table S1. Enrichment analysis for proteins encoding signal sequences in the exo-proteome. Proteins encoding signal sequences were predicted using data from the Joint Genome Institute's Integrated Microbial Genomes (JGI-IGM) database (Chen *et al.*, 2017) and prediction programs SignalP (Petersen *et al.*, 2011), Phobius (Kall *et al.*, 2007), SecretomeP (Bendtsen *et al.*, 2005), Tatfind (Dilks *et al.*, 2003), PilFind (Imam *et al.*, 2011) and SSPRED (Pundhir and Kumar, 2011), which predicts specific classes of signal peptides. P-values were calculated using the one-sided Fisher's exact test, with p-values $\leq$0.05 highlighted.

Table S2. Biofilm development by sedimenting mutants. Biofilm forming strains are indicated in green. Transposon insertional inactivation was performed using the indicated vectors from the unigene set (UGS) library or the Golden lab's private library set (Holtman *et al.*, 2005; Chen Y, 2012). In cases where two genes are indicated the insertion is in the intergenic region.

Table S3. Summary of molecular manipulations. Gene deletion vectors were initially constructed by cloning into pJET1.2 a PCR product amplified with the indicated primers. Subsequently, the indicated restriction sites were used for deletion and insertion of either kanamycin or gentamicin resistance cassettes, as indicated. Transposon insertional inactivation was performed using the indicated vectors from the unigene set (UGS) library (Holtman *et al.*, 2005; Chen Y, 2012). Gene disruption in *S. elongatus* was obtained by transformation and replacement of the native gene by homologous recombination. Complementation of T2SEΩ was performed by introduction of a copy of the 2071 ORF with its native promoter region into neutral site I using a vector constructed by seamless assembly of this amplicon into SwaI-digested pCV0063, a neutral site I cloning vector (Taton *et al.*, 2014). Data for complementation of PilA2 and T2SEΩ are provided in Fig. S1B and S1C. The phenotype of mutant PilA1 was observed following multiple independent insertional inactivations.

Figure S1. A. Cultures of T2SEΩ and PilA2 strains (7d old). Cells of these strains adhere to the glass tube, apparently in large clusters of cells. B and C. Chlorophyll in suspended cells in 7d old cultures of wild type (WT), T2SEΩ, PilA2 mutant and the complemented strains of these mutants (PilA2/comp and T2SEΩ/comp, respectively). For further details of complementation see Table S3. Graph shows averages and standard deviations of three technical repeats. Phenotypic complementation of these mutants was observed in three independent biological repeats.

Figure S2. A. Maps of the genomic regions of *pilA*-candidate genes, the inactivation of which did not result in biofilm formation. Asterisks denote the transposon insertion site. The fragment between the *BlpI* and *BsgI* was deleted. B. Chlorophyll in suspended cells in 7d old cultures of wild type (WT), T2SEΩ, mutants obtained following insertional inactivation of Synpcc7942_2482 (2482Ω), Synpcc7942_2484 (2484Ω) and Synpcc7942_2485 (2485Ω) as well as a strain in which Synpcc7942_2590 and Synpcc7942_2591 were deleted (2590/2591Δ).

Figure S3. Schematic of the custom-made flow cell for the deposition studies.